IAC-25-C2.1.7.x100743

Design, Analysis and Comparison of Biomimetic Hierarchical Honeycomb Sandwich Composites for Aerospace Applications

Dinendra Arcot Viswanath[a]*, Dr. Antonio Mattia Grande[b], Akshayanivasini Ramasamy Saravanaraj[c]

[a] *Department of Aerospace Engineering, Politecnico di Milano, Piazza Leonardo da Vinci 32, Milan, Italy.* Email: dinendra.arcotviswanath@gmail.com

[b] *Associate Professor, Department of Aerospace Engineering, Politecnico di Milano, Piazza Leonardo da Vinci 32, Milan, Italy.* Email: antoniomattia.grande@polimi.it

[c] *Department of Aerospace Engineering, Politecnico di Milano, Piazza Leonardo da Vinci 32, Milan, Italy.* Email: akshayanivasini.sr@gmail.com

* Corresponding author

Abstract

This study explores the performance of a geometrically modified honeycomb structure in terms of crashworthiness, energy absorption capacity, and structural stiffness, through a comparative analysis with a conventional honeycomb core design. To evaluate the influence of hierarchical geometry on these parameters, three distinct honeycomb core models were developed, each representing an ascending level of hierarchical complexity. The hierarchical architecture, inspired by spider web morphology, integrates smaller hexagonal infill patterns concentrically within the primary honeycomb cells. These nested hexagons are connected via radial spoke-like beams, mimicking the concentric and radial organization characteristic of natural spider webs. The geometric models for all configurations were developed using SolidWorks. A standard hexagonal honeycomb core was also created to serve as a baseline for comparison. All core models were subjected to identical boundary conditions and loading scenarios to ensure consistency and accuracy across simulations. Finite element simulations were conducted using ANSYS Mechanical Workbench and ANSYS Mechanical LS-DYNA 2023 R1. For crashworthiness evaluation, an out-of-plane impact loading scenario was simulated. For stiffness evaluation, Aluminium 7075-T6 (Al 7075-T6) honeycomb cores were sandwiched in between two Carbon Fibre Reinforced - Polyether Ether Ketone (CFR-PEEK) face sheets and the assembled specimens were subjected to three-point bending tests to evaluate their specific stiffness and flexural rigidity. These sandwich composite specimens were developed due to their widespread adoption in the aerospace industry, where high stiffness-to-weight ratios are essential. Additionally, low-velocity drop-weight impact tests were carried out to assess the structures' energy absorption characteristics. The simulation results indicate that hierarchical honeycomb cores offer significantly improved mechanical performance compared to the conventional design—particularly in terms of energy absorption and stiffness. This enhancement is attributed to the added geometric complexity of the hierarchical structuring, which plays a key role in optimizing structural response under both quasi-static and dynamic loading. These findings underscore the promise of biomimetic hierarchical designs in advancing lightweight structural systems for high-performance aerospace applications.

Keywords

Hierarchical honeycomb cores, Crashworthiness, Energy absorption, Specific stiffness, Finite element simulations, Biomimetic

Acronyms/Abbreviations

$CFR-PEEK$ = Carbon Fibre Reinforced - Polyether Ether Ketone

RHC = Regular Honeycomb Core

HHC = Hierarchical Honeycomb Core

SEA = Specific Energy Absorption $[kJ/kg]$

PCF = Peak Crushing Force $[N]$

MCF = Mean Crushing Force $[N]$

Nomenclature

ρ = Density $[kg/m^3]$

ρ_{rel} = Relative density

$\bar{\rho_r}$ = Relative density of Regular Honeycomb Core

$\bar{\rho_f}$ = Relative density of First Order Hierarchical Honeycomb Core

$\bar{\rho_s}$ = Relative density of Second Order Hierarchical Honeycomb Core

δ = Displacement $[m]$

δ_f = Final Displacement $[m]$

ρ^* = Effective density $[kg/m^3]$

ρ_{web} = Relative density of the web

ρ_{fill} = Relative density of the solid fill area

$\rho_{overlap}$ = Relative density of the overlap region

λ_i = Hierarchical parameter; i refers to the order

L = Span length $[m]$

l = Cell wall length $[m]$

t_r = Wall Thickness of Regular Honeycomb $[m]$

t_f = Wall Thickness of First order Honeycomb $[m]$

t_s = Wall Thickness of Second order Honeycomb $[m]$

b = Breadth of the specimen $[m]$

h = Height of the specimen$[m]$

m = Slope of the Linear elastic region

M = Mass of the specimen $[kg]$

E_f = Flexural modulus $[GPa]$

D = Flexural rigidity $[Nm^2]$

E_{total} = Total energy absorbed $[kJ]$

I = Area moment of inertia $[m^4]$

k = Stiffness of the specimen $[kN/m]$

k_s = Specific Stiffness of the specimen $[MJ/kg]$

1. Introduction

Kinetic energy absorption is a central challenge in aerospace engineering, where spacecraft and aircraft structures are exposed to demanding conditions such as high-velocity debris [1] [2] [3],intense launch vibrations, and docking or landing shocks. Without effective dissipation mechanisms, these loads can lead to catastrophic structural failure, instrument malfunction, or even mission loss. The ability to combine high load-bearing capacity with minimal mass is therefore fundamental to modern aerospace design, driving the search for structural concepts that are both lightweight and mechanically robust.

Conventional honeycomb cores have long been a preferred choice in this pursuit, valued for their geometric efficiency and excellent strength-to-weight ratio. The hexagonal cell structure distributes stresses evenly and allows for substantial weight reduction, making these cores widely adopted in aerospace applications ranging from fuselage panels to satellite structures. Yet, under dynamic and impact loading, their limitations become apparent. Thin cell walls are susceptible to localized stress concentrations and premature buckling, which reduce their energy absorption capacity and compromise crashworthiness. These shortcomings restrict their performance in scenarios where controlled deformation and high energy dissipation are critical.

To overcome these limitations, a variety of alternatives such as foam-filled cores, lattice or truss-based systems, and hybrid composites have been investigated. While each has demonstrated improvements in stiffness or impact resistance, they are often associated with trade-offs, including additional mass, manufacturing complexity, or reduced scalability for aerospace applications. Against this backdrop, hierarchical honeycomb composites represent a promising advancement [4] [5]. By embedding smaller-scale substructures within the primary honeycomb framework, they maintain the lightweight efficiency of traditional designs while offering enhanced stiffness, improved load redistribution, and greater crash resistance. However, despite these promising characteristics, current research into hierarchical cores remains relatively limited, with most findings derived from simulations or small-scale studies. Addressing this gap through systematic investigation is essential to assess their viability as an alternative or complement to existing core architectures in advanced aerospace structures.

1.1 Biomimicry in Aerospace

Biomimicry—the adoption of nature's optimized structural solutions—offers a promising pathway to meet the dual demands of lightness and strength [6] [7] [4]. Bird wings inspire aerodynamic wing and winglet profiles, shark skin textures reduce drag, termite mound ventilation informs passive thermal regulation, and beetle shells guide thermal protection for atmospheric re-entry. Among these natural designs, the hexagonal geometry of honeycombs stands out for its strength-to-weight efficiency. Honeycomb composites are widely used in aerospace because their hexagonal cell arrangement distributes stress evenly, resists deformation, and remains lightweight. Recent advances have introduced hierarchical honeycombs, where smaller-scale honeycomb networks are embedded within larger cells to optimize load transfer, reduce stress concentrations, and improve stiffness and strength beyond conventional designs. The hierarchical configurations also allow for precise control of elastic buckling behavior, enhancing both energy absorption and structural support. Vertex-based hierarchical designs have been shown to improve specific energy absorption and load-carrying ability, making them highly suitable for impact-resistant aerospace applications.

1.2 Tensegrity Principles and Spider Web Architecture

Another remarkable natural model for energy absorption is the spider web. Despite its minimal material use, a web can sustain significant forces through its strategic geometry and mechanical properties. Radial threads form the primary load-bearing framework, while spiral threads—often arranged according to logarithmic and arithmetic spiral patterns—provide elasticity, absorbing and dissipating impact energy. The pre-tensioned configuration preserves stability, delays slackening, and prevents nonlinear deformation, while redundancy ensures functionality even after partial damage. Radial line thickness has been found to correlate positively with specific energy absorption, further contributing to the web's mechanical efficiency [8] [9] [10]. This performance is rooted in the principle of tensegrity—short for "tensional integrity"—in which pre-tensioned tensile members work in conjunction with isolated compression components to achieve exceptional strength-to-weight ratios, flexibility, and efficient stress distribution.

1.3 Conceptual Synthesis of Spider Webs and Honeycombs

This study proposes a novel aerospace structural concept that merges the energy-dissipating capabilities of spider web tensegrity with the structural efficiency of hierarchical honeycombs. In this design, each hexagonal cell of a hierarchical honeycomb core incorporates a web-inspired geometry, creating a hybrid sandwich composite. Corner-enhanced spider web honeycombs are used to improve both energy absorption and deformation characteristics, ensuring equal loading on both sides of the honeycomb wall and central node—an effect that also reflects the stiffness characteristics of natural spider silk. By uniting the honeycomb's material efficiency with the web's dynamic load management, this composite aims to deliver ultralight, high-strength aerospace components capable of meeting the extreme mechanical demands of space missions.

2. Material and methods

2.1 Geometric Modelling

To facilitate a structured comparison, the core configurations were designated using a consistent naming scheme. The regular honeycomb core is referred to as **RHC** (Regular Honeycomb Core), while the hierarchical variants are denoted as **HHC-X**, where *X* indicates the order of hierarchy introduced within the cellular structure. Accordingly, **HHC-1**, **HHC-2**, and **HHC-3** represent the first, second, and third-order hierarchical honeycomb cores, respectively.

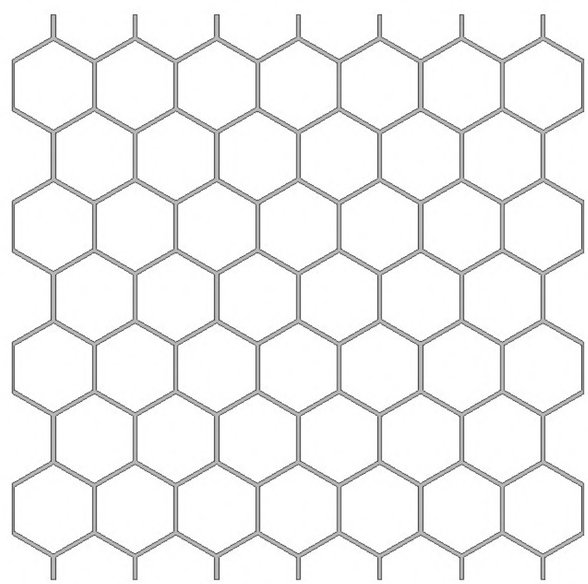

Fig. 1: Top view of RHC

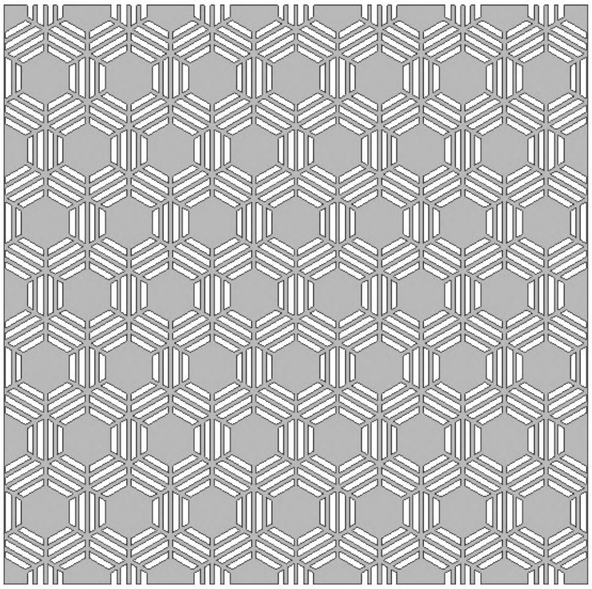

Fig. 2: Top view of HHC-1

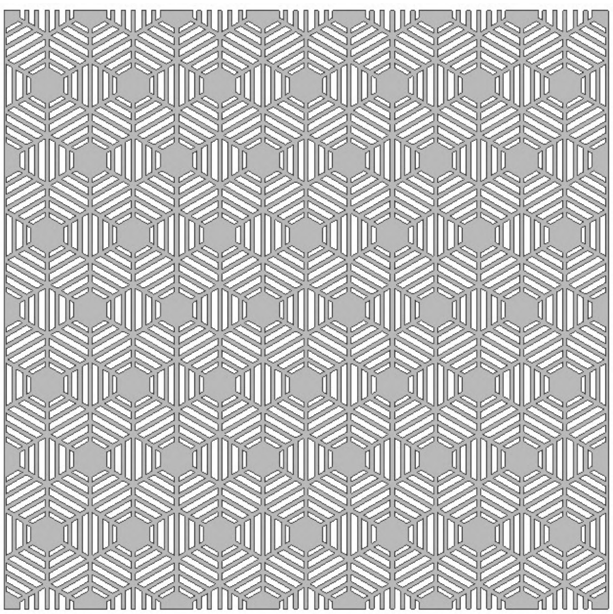

Fig. 3: Top view of HHC-2

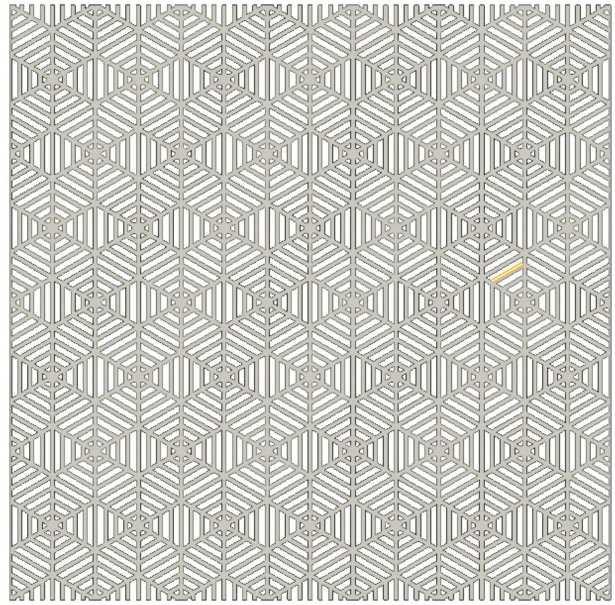

Fig. 4: Top view of HHC-3

The baseline configuration, RHC, was modelled with a cell diameter of 10 mm and a wall thickness of 1 mm. Hierarchical cores were developed in ascending levels of complexity by embedding additional substructures within the parent cell geometry. This progressive modification allowed for a systematic investigation into the influence of hierarchical order on the mechanical response of the cores under loading.

While natural spider webs exhibit radial arrangements governed by the Fibonacci sequence [8], the hierarchical infill patterns in this study were designed with equal radial spacing to reduce geometric complexity while promoting uniform stress distribution under loading. For HHC-1, the infill cell diameter was 8 mm; for HHC-2, 5 mm; and for HHC-3, 3 mm. In all hierarchical configurations, the radial spokes were assigned the same thickness as the honeycomb cell walls to maintain geometric uniformity and consistent stiffness properties.

The overall core dimensions were adapted according to the type of numerical analysis performed. For crashworthiness simulations, the core was modelled with a length of 75 mm and a thickness of 10 mm. For flexural simulations, the core length was increased to 150 mm while the thickness was reduced to 0.5 mm to accommodate the three-point bending configuration.

In the flexural analysis, the sandwich composite specimen incorporated homogeneous solid face sheets with plan dimensions of 150 mm × 73 mm and a thickness of 1 mm each, yielding a total composite thickness of 2.5 mm when combined with the core. The top views of the RHC, HHC-1, HHC-2 and HHC-3 are displayed above in Figures 1, 2, 3 and 4 respectively.

2.2 Relative and Effective density Calculation

The relative density of the honeycomb is essential for evaluating the performance of the cores as it provides the basis for calculating energy absorption efficiency. The relative density of the hierarchical honeycombs was determined following the relations proposed by He, Qiang, *et al.* [11], where the geometry of the refined sub-cells is incorporated into the density expression through the hierarchical parameters. For the regular, first-order, and second-order configurations, the relative densities are expressed as:

$$\bar{\rho}_r = \frac{2}{\sqrt{3}} \cdot \frac{t_r}{l}, \tag{1}$$

$$\bar{\rho}_f = \frac{6}{\sqrt{3}} \cdot \frac{t_f}{l}, \tag{2}$$

$$\bar{\rho}_s = \frac{2}{\sqrt{3}} \cdot \frac{t_s}{l(3+2\lambda_i)}. \tag{3}$$

Here, t_r, t_f, and t_s denote the effective wall thicknesses of the regular, first-order, and second-order honeycomb structures, respectively, while l represents the cell wall length and λ_i is the hierarchical parameter. In the present study, these expressions were adapted with minor modifications to account for the specific geometry of the proposed hierarchical patterns.

Although these relations were adopted as the baseline, the geometric configuration employed in this study differed significantly from that of the reference literature. To account for the solid-filled region at the center of the infill pattern, the density of the infill area and an additional overlap margin were introduced. To determine the relative density of HHC-3, the $\bar{\rho_s}$ expression was extrapolated. The total relative density of the configuration was then expressed as:

$$\rho_{rel} = \rho_{web} + \rho_{fill} - \rho_{overlap} \tag{4}$$

The effective density of the cellular structure is obtained as:

$$\rho^* = \rho_{rel} \cdot \rho_m \tag{5}$$

where ρ_{rel} is the relative density of the honeycomb and ρ_m is the density of the material. The effective densities of the RHC, HHC-1, HHC-2, and HHC-3 were calculated as 339.66 kg/m^3, 1906.72 kg/m^3, 1387.69 kg/m^3 and 1093.73 kg/m^3 respectively.

2.3 Materials

The honeycomb core was assigned the Aluminium alloy 7075-T6 (Al 7075-T6). Al 7075-T6 was selected for its high tensile and shear strength, elevated yield strength, and excellent strength-to-weight ratio, ensuring structural integrity under significant loads while maintaining low mass [12] [13] [14] [15].

Table 1: Mechanical properties of Al 7075 T6 and CFR-PEEK.

Property	Symbol	Al 7075 T6	CFR-PEEK
Density (kg/m^3)	ρ	2810	1380
Young's Modulus (MPa)	E	71700	6000
Shear Modulus (MPa)	G	26900	6100
Tensile Strength (MPa)	σ_t	503	112
Flexural Strength (MPa)	σ_f	331	184
Poisson Ratio	ν	0.33	0.28

For the face sheets of the sandwich composite specimen, Carbon Fibre Reinforced - Polyether Ether Ketone (CFR-PEEK) was assigned. CFR-PEEK was chosen for its exceptional tensile stiffness, impact toughness, fatigue resistance, and thermal stability, which are critical for withstanding extreme aerospace environments [16] [17] [18] [19]. The Material properties for both constituents were obtained from various literature and verified against manufacturer data sheets to ensure accuracy in the numerical simulations.

2.4 Finite Element Modelling

All numerical simulations were performed in ANSYS 2023 R1, particularly the impact loading numerical simulations were performed in ANSYS Mechanical LS-DYNA and the flexural analysis simulations in ANSYS Workbench.

2.4.1 Out of plane impact loading analysis

The Honeycomb Cores were evaluated under axial crushing conditions using ANSYS Mechanical LS-DYNA. The setup model is illustrated in Figure 5. Each core was positioned between two rigid surfaces, with the lower surface fixed as a rigid wall and the upper surface functioning as the rigid impactor. The honeycomb cores were discretized with solid elements, while the rigid wall and impactor were modelled with shell elements. A mesh size of 0.6 mm was assigned to the core, and 1 mm to the rigid surfaces. The cores were assigned Aluminium alloy 7075-T6 properties, incorporating a Johnson–Cook strength and failure model for plasticity and isotropic elasticity for elastic behaviour. Contact between the rigid surfaces and the core was defined using an automatic node-to-surface frictional contact, with static and dynamic friction coefficients of 0.3 and 0.2, respectively.

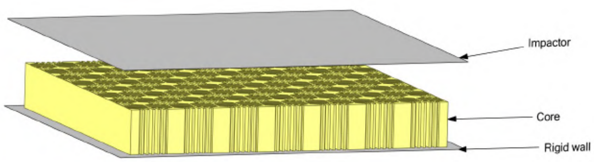

Fig. 5: Impact loading simulation setup

All bottom edges of the cores were fully constrained, while the vertical edges were restricted in all degrees of freedom except translation along the Y-axis for uniform and progressive crushing behaviour. An attached mass of 400 kg and an initial velocity of 15 m/s along the negative Y-direction were applied to the rigid impactor as boundary conditions. This setup was used consistently across all test specimens in the impact analysis [11].

2.4.2 Three point bending analysis

A three-point bending flexural analysis was conducted on the sandwich composite specimen using ANSYS Workbench [20] [21] and the test setup is shown in the Figure 6.

The composite panel, with an overall thickness of 2.5 mm, was placed on support rollers, while a loading anvil was placed at the mid-span of the specimen. Both the loading and support anvils were modelled and assembled in ANSYS SpaceClaim 2023. The supports were located 20 mm from each end, resulting in a total span length of 120 mm.

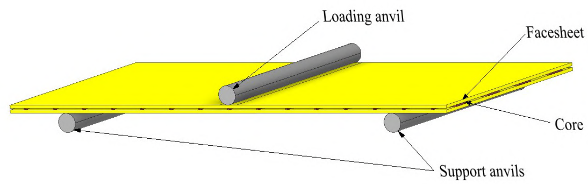

Fig. 6: Three point bending simulation setup

Both the sandwich composite core and the face sheets were meshed with solid elements. A global element size of 1 mm was applied to the core and 3 mm to the face sheets, ensuring adequate resolution of local stress and deformation behaviour. The contact between the loading anvil and the specimen was defined as frictional with a coefficient of 0.1, whereas the contact between the bottom face sheet and the support anvils was defined as frictionless. Remote displacement boundary conditions were applied, with the support rollers fully constrained in all six degrees of freedom and the loading anvil prescribed a displacement of –15 mm along the negative Y-axis. The numerical analysis was executed in 30 load steps to capture the progressive flexural response of the specimen.This setup was used consistently across all test specimens in the flexural analysis simulations [22] [23] [24] [25].

3. Performance metrics and Governing equations

3.1 Crashworthiness Parameters

To evaluate the crashworthiness of hierarchical honeycomb structures, The specific energy absorption (SEA), representing the energy absorbed per unit mass [11], was calculated using

$$SEA = \frac{E_{\text{total}}}{M} = \frac{1}{M}\int_0^{\delta_f} F(\delta)\, d\delta, \tag{6}$$

where d is the compression displacement, M is the mass of the honeycomb specimen, E_{total} represents the total energy absorbed throughout the crushing process, and $F(\delta)$ is the axial force as a function of the displacement. The peak crushing force (PCF), indicating the maximum instantaneous load, was determined as

$$PCF = \max(F(\delta)), \tag{7}$$

and the mean crushing force (MCF), representing the average load during the crushing process, was calculated by

$$MCF = \frac{E_{\text{total}}}{\delta_f}. \tag{8}$$

These parameters collectively provide a comprehensive framework to assess the crashworthiness performance of hierarchical honeycomb structures, enabling comparison between different geometries and optimization for lightweight, energy-absorbing applications.

3.2 Flexural Analysis Parameters

To evaluate the bending behavior of honeycomb sandwich composites, several key flexural parameters were determined, including flexural modulus, flexural stiffness, and specific flexural stiffness [26] [25]. These metrics allow evaluation of both the intrinsic material properties and the performance of the panel as a structural element.

The **flexural modulus**, E_f, quantifies the panel's resistance to elastic deformation and is obtained from the slope of the initial linear portion of the load–deflection curve:

$$E_f = \frac{L^3 m}{4bh^3} \tag{9}$$

where m is the slope of the linear elastic region. This parameter indicates the stiffness of the material and enables prediction of the panel's deflection under applied loads.

The **flexural stiffness** or flexural rigidity, D, describes the structural resistance of the panel to bending and is defined as

$$D = E_f I = \frac{L^3 m}{48} \tag{10}$$

where I is the second moment of area. Higher bending rigidity corresponds to lower deflection for a given load, reflecting the panel's overall structural performance.

Finally, the **specific stiffness**, k_s, evaluates the efficiency of the panel with respect to weight and is expressed as

$$k_s = \frac{E_f}{\rho^*} \tag{11}$$

where ρ^* is the effective density of the sandwich panel. This parameter is particularly important in aerospace applications, as it allows comparison of different designs not only by stiffness but also by how effectively stiffness is achieved relative to mass.

These parameters collectively describe the bending behavior of the honeycomb sandwich panels and enable direct comparison of different core designs in terms of both performance and weight efficiency.

4. Results and Discussions

4.1 Flexural data analysis

4.1.1 Stress Distribution of the cores

The following figures illustrate the stress distribution across the deformed core regions,

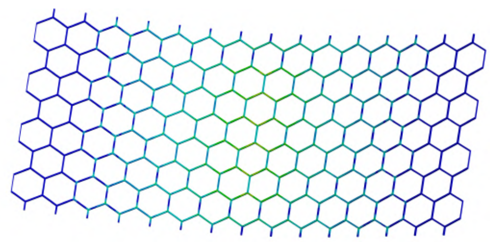

Fig. 7: Core deformation of RHC

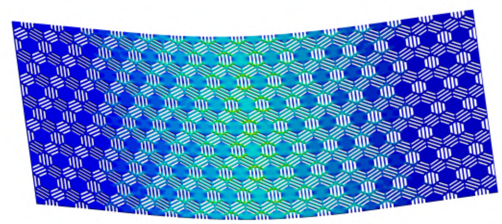

Fig. 8: Core deformation of HHC-1

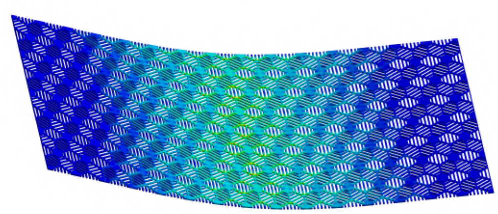

Fig. 9: Core deformation of HHC-2

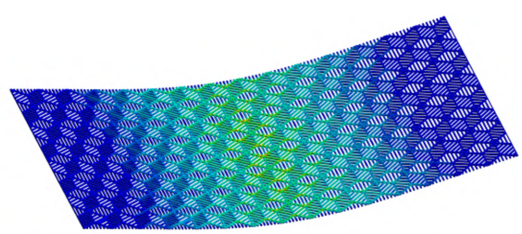

Fig. 10: Core deformation of HHC-3

Although the stress distribution patterns across the core variants appear generally similar in form, distinct differences emerge in terms of stress intensity and spread with increasing hierarchical complexity. HHC-3 demonstrates the most extensive stress distribution, while RHC exhibits a more localized stress profile Figure 11. The maximum stress values sustained by RHC, HHC-1, HHC-2, and HHC-3 are (insert values), respectively, with HHC-3 enduring the highest and RHC the lowest. Taken together, this trend underscores the role of hierarchical structuring in facilitating more effective load transfer and distribution within the core.

Although the global stress distribution in HHC-3 has improved markedly, regions of elevated stress concentration are evident at the web junctions, as indicated by localized red zones in the contour plots. These concentrations are more pronounced in HHC-3 Figure 10 compared to HHC-2 Figure 9, where the stress at these junctions is moderately reduced. In HHC-1 Figure 8, this effect is further alleviated; however, the overall area over which stress is distributed is comparatively smaller than in HHC-2. The increased stress concentration in HHC-3 can be attributed to the reduced joint interface area between the central web and the intersecting webs, which limits the load sharing capacity at these junctions. As a result, applied stress is transferred through narrower paths, leading to higher localized stresses despite the overall improvement in global distribution.

4.1.2 Flexural parameters comparison

The flexural properties of the RHC and HHC specimens were evaluated in terms of stiffness, flexural modulus, flexural rigidity, and specific stiffness. The results reveal notable improvements in mechanical performance for the HHC specimens compared to the RHC. Table 1 provides the flexural parameters of the Sandwich composite specimens for comparison.

Table 2: Flexural properties of Sandwich composite variants

Specimen	k (kN/m)	E_f (GPa)	D (Nm^2)	k_s (MJ/kg)
RHC	68.5	24.5	2.32	20.86
HHC-1	96.2	34.3	3.25	23.12
HHC-2	92.07	32.9	3.11	23.79
HHC-3	91.55	32.7	3.1	24.70

In terms of stiffness, all HHC specimens exhibited significantly higher values compared to RHC. HHC-1 recorded the highest stiffness at 96.2 kN/m, followed by HHC-2 (92.07 kN/m) and HHC-3 (91.55 kN/m). In contrast, RHC demonstrated the lowest stiffness at 68.5 kN/m, indicating a less rigid structural response under loading. This overall increase in stiffness across the HHC variants can be attributed to hierarchical structural enhancements. Specifically, the superior stiffness and flexural rigidity observed in HHC-1 are likely due to the relatively larger material area and central web cross-section compared to the other specimens, which facilitates more efficient load transfer and greater structural integrity.

A similar trend is observed in the flexural modulus (E_f). HHC-1 exhibited the highest modulus at 34.3 GPa, suggesting improved resistance to bending deformations. HHC-2 and HHC-3 followed closely with values of 32.9 GPa and 32.7 GPa, respectively. RHC again presented the lowest modulus at 24.5 GPa, reinforcing the observation of its comparatively lower stiffness at the material level. These results support the conclusion that hybrid composite configurations contribute positively to the flexural stiffness of the overall matrix.

Flexural rigidity (D), which accounts for both the material stiffness and geometric moment of inertia, was highest in HHC-1 at 3.25 N·m^2. HHC-2 and HHC-3 exhibited slightly lower but comparable values of 3.11 and 3.10 N·m^2, respectively. RHC, by contrast, displayed a significantly lower rigidity of 2.32 N·m^2. The improved flexural rigidity of the HHC variants highlights their structural advantage in applications where resistance to bending is critical.

Notably, specific stiffness (k_s), which normalizes absolute stiffness with respect to weight, was highest in HHC-3 at 24.70 MJ/kg. This was followed by HHC-2 (23.79 MJ/kg) and HHC-1 (23.12 MJ/kg), while RHC recorded the lowest value at 20.86 MJ/kg. Although HHC-1 achieved the highest absolute stiffness, the superior stiffness-to-weight ratio observed in HHC-3 suggests its potential suitability in weight-sensitive structural applications.

Collectively, the data indicate that all HHC specimens outperform the RHC configuration across the evaluated mechanical parameters. Among the hybrids, HHC-1 offers the greatest stiffness and rigidity, while HHC-3 demonstrates the most favorable specific stiffness.

4.1.3 Influence of Hierarchical patterns

The comparative analysis between the RHC and HHC specimens highlights the significant role of hierarchical structuring in enhancing the mechanical performance of sandwich composites. The hierarchical configurations present in the HHC variants contribute to marked improvements in stiffness, flexural modulus, and rigidity when compared to the baseline RHC specimen.

These improvements are attributed to the ability of hierarchical architectures to redistribute mechanical loads more efficiently, thereby minimizing localized stress concentrations. The stress flow through multi-scale paths in the hierarchical structures leads to improved structural synergy, which in turn enhances load-bearing capacity without a proportional increase in material usage.

Among the HHC variants, HHC-3 stands out with the highest specific stiffness, demonstrating the effectiveness of hierarchical design not only in absolute performance, but also in stiffness-to-weight optimization. The presence of branching or layered reinforcement patterns within the HHC structures enables greater energy absorption and delayed failure initiation, which are critical for flexural applications.

These results clearly demonstrate that the inclusion of hierarchical features strengthens the overall structure, leading to a more mechanically efficient composite.

4.2 Impact data Analysis

4.2.1 Deformation of the cores

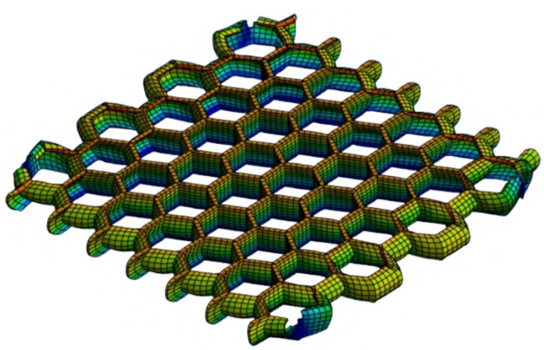

Fig. 11: Deformed RHC after impact

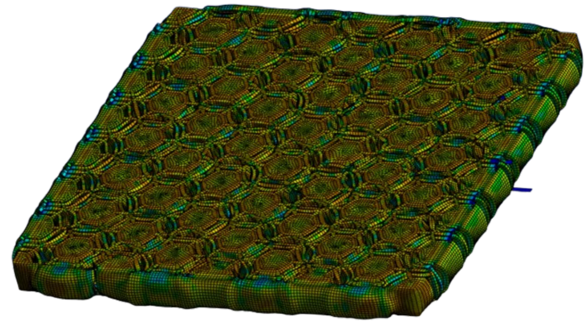

Fig. 12: Deformed HHC-1 after impact

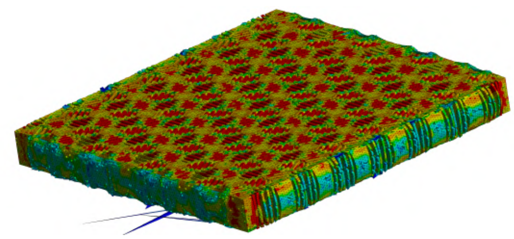

Fig. 13: Deformed HHC-2 after impact

Fig. 14: Deformed HHC-3 after impact

From the images, it is observed that the Regular Honeycomb core has buckled more than the hierarchical honeycomb cores significantly. Though the hierarchical honeycomb cores have buckled less, the webs started to break in the HHC-2 and HHC-3. This maybe due to the smaller areas of the hexagons at the center of the infill pattern which provided a smaller bonding area between the center and the webs. Despite this, the total compression distance of the HHCs reduces as the complexity of the hierarchy increases. This maybe due to the buckling of the internal walls within the honeycomb cell which causes the parallel walls come into contact with each other and prevents the total collapse of the structure.

4.2.2 Crashworthiness metrics comparison

The crashworthiness metrics namely, the Specific Energy Absorption (SEA) and the Peak Crushing Force (PCF) are derived from the force-displacement data extracted from the impact simulation results. Table 2 below showcases the comparison of the metrics for all test specimens.

Table 3: Crashworthiness performance metrics of different core configurations

Specimen	SEA (kJ/kg)	PCF (MN)	MCF (MN)
RHC	189.17	1.1744	0.455
HHC-1	170.75	5.9571	4.89
HHC-2	310.26	5.1	4.23
HHC-3	423.53	4.788	4.34

The crashworthiness characteristics of the examined specimens were evaluated with reference to specific energy absorption (SEA), peak crushing force (PCF), and mean crushing force (MCF). Among the configurations, HHC-3 (Figure 14) exhibited the highest energy absorption efficiency, attaining a value of 423.53 kJ/kg, which is more than double that of the reference specimen RHC (189.17 kJ/kg). HHC-2 (Figure 13) also demonstrated a comparatively strong performance, recording a SEA of 310.36 kJ/kg, whereas HHC-1 (Figure 12) displayed the lowest energy absorption capacity (170.75 kJ/kg), marginally below that of RHC (Figure 11) . These findings underscore the markedly superior capacity of the HHC-3 configuration to dissipate impact energy relative to the other specimens under investigation.

With respect to Peak crushing force, RHC registered the lowest value (1.1744 MN), thereby evidencing its effectiveness in limiting peak impact loads. In contrast, HHC-1 exhibited the highest PCF (5.96 MN), signifying a greater propensity to transmit elevated instantaneous forces during crushing. The remaining hybrid specimens, HHC-2 and HHC-3, produced intermediate PCF values of 5.10 MN and 4.79 MN, respectively, which indicates partial improvement in mitigating peak load compared with HHC-1, though both remained substantially higher than RHC. In terms of mean crushing force, HHC-1 attained the highest sustained resistance (4.89 MN), followed in close succession by HHC-3 (4.34 MN) and HHC-2 (4.23 MN). RHC, by contrast, exhibited a markedly lower mean force of 0.455 MN, highlighting its limited capacity to endure progressive crushing. Taken together, these observations establish that the hybrid configurations (HHC series) provide considerably enhanced structural robustness relative to the reference specimen.

The comparative analysis reveals clear distinctions in performance behavior among the investigated specimens. The RHC specimen demonstrates effectiveness in reducing peak forces; however, its low energy absorption and insufficient load-bearing capability substantially restrict its overall crashworthiness. HHC-1, while capable of sustaining the highest mean crushing force, does so at the cost of elevated peak forces and comparatively reduced SEA, thereby limiting its energy absorption efficiency. HHC-2 exhibits a more balanced performance profile, combining relatively high SEA with moderate peak force and adequate mean force resistance. HHC-3 emerges as the most advantageous configuration, combining exceptional energy absorption with stable mean crushing resistance and a lower peak force than that recorded for HHC-1.

In summary, HHC-3 is identified as the most effective energy-absorbing configuration and, accordingly, the most suitable for applications requiring crash energy dissipation. The RHC specimen, although advantageous where minimization of peak impact forces is prioritized, is constrained by its inadequate energy absorption capability, which limits its functional applicability. HHC-2 constitutes a balanced compromise, providing an advantageous combination of energy absorption efficiency and load management. By comparison, HHC-1, despite its notable load bearing strength, is penalized by reduced energy absorption efficiency and an elevated peak force response, both of which detract from its overall effectiveness.

4.3 Overall Comparison

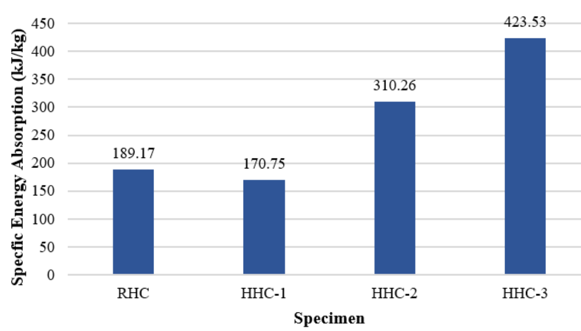

Fig. 15: Specific Energy Absorption Comparison Chart

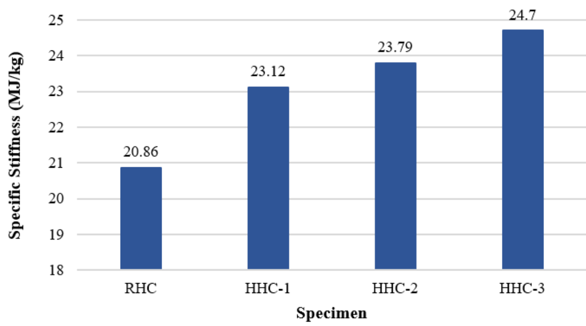

Fig. 16: Specific Stiffness Comparison Chart

The comparison between the regular honeycomb core (RHC) and the hierarchical honeycomb cores (HHC) underscores the clear benefits of hierarchical structuring in improving the mechanical efficiency of sandwich composites. Across all measured parameters, the HHC configurations consistently outperformed the RHC, demonstrating their ability to enhance both strength and energy absorption through more effective load distribution. The Comparison graphs of specific energy absorption and specific stiffness, along with the corresponding specimens, are presented above in Figures 15 and 16.

In terms of flexural behavior, all HHC variants exhibited higher stiffness, modulus, and rigidity than the RHC specimen. HHC-1 achieved the highest absolute stiffness (96.2 kN/m) and flexural rigidity (3.25 N·m²), a result attributed to its relatively larger central web geometry, which increased the moment of inertia and facilitated more efficient load transfer. HHC-3, while slightly lower in absolute stiffness, attained the highest specific stiffness (24.70 MJ/kg), reflecting its ability to provide a more favorable stiffness-to-weight balance. This distinction is particularly important for weight-sensitive applications, where material efficiency is often as critical as absolute strength. HHC-2, although stronger than the RHC, occupied an intermediate position: its flexural performance was solid but did not exceed HHC-1 in absolute values or HHC-3 in normalized efficiency, limiting its competitiveness as a preferred option.

Impact behavior provided further confirmation of these observations. The RHC specimen was highly susceptible to buckling under load, showing limited capacity to maintain structural integrity. In contrast, the hierarchical cores resisted collapse more effectively, with their multi-scale layouts enabling stresses to be redistributed through several internal pathways. Although HHC-2 and HHC-3 exhibited localized web breakage, likely a consequence of smaller bonding areas in their central cells, this did not compromise overall stability. Instead, the interactions between adjacent internal walls helped delay the full collapse and reduced the extent of deformation. As a result, both HHC-2 and HHC-3 achieved markedly higher specific energy absorption values, reaching 310.26 kJ/kg and 423.53 kJ/kg, respectively. HHC-1 distinguished itself differently, recording the highest peak crushing force (5.96 MN),highlighting its capacity to withstand greater instantaneous loading.

Together, these results highlight the clear advantages of hierarchical configurations over the regular honeycomb core. HHC-1 demonstrates the highest stiffness and rigidity, though this performance primarily arises from its greater material content and associated weight, rather than superior structural efficiency. In contrast, HHC-3 offers the strongest overall balance of structural strength, weight efficiency, and crashworthiness.

The demonstrated improvements also highlight the strong potential of hierarchical honeycomb cores in aerospace and space applications. Their combination of high stiffness, rigidity, and load bearing capacity makes them well suited for demanding structural elements such as aircraft fuselage panels, satellite bus structures, and launch vehicle fairings. At the same time, their favorable stiffness-to-weight balance and reliable crashworthiness performance underline their suitability for spacecraft panels, deployable structures, and protective shielding, where minimizing mass is essential without compromising mechanical integrity.

5. Conclusion

This study has shown that hierarchical honeycomb cores offer clear advantages over the regular honeycomb configuration in improving the mechanical efficiency of sandwich composites. The hierarchical designs consistently achieved higher stiffness, flexural rigidity, and energy absorption, reflecting their ability to distribute loads more effectively and maintain structural stability under impact. Among the configurations, HHC-3 provided the most balanced performance in terms of strength, weight efficiency, and crashworthiness, while HHC-2 is noteworthy for exhibiting performance closely comparable to HHC-3, with the only distinction being a marginal increase in weight.

In summary, the results establish hierarchical architectures as a more effective alternative to conventional cores, supporting their use in the development of lightweight structural systems where both strength and efficiency are critical. Future work will involve the fabrication of prototypes through additive manufacturing, followed by experimental testing to evaluate their structural integrity and thermal expansion behavior. These results will guide the optimization of geometric parameters, such as cell size and web thickness, to tailor the structures for specific application requirements.

Acknowledgements

I sincerely thank the **Department of Aerospace Engineering** at **Madras Institute of Technology (MIT), Anna University, Chennai, India** for enabling my student exchange program, which allowed me to complete the final year of my Master's at **Politecnico di Milano** and defend my thesis, without which this research could not have been undertaken. I also appreciate my department for providing access to essential computer lab facilities, including the ANSYS software, which were crucial for the simulations in this study.

References

[1] William Schonberg, Frank Schäfer, and Robin Putzar. Hypervelocity impact response of honeycomb sandwich panels. *Acta Astronautica*, 66:455–466, 02 2010.

[2] Yanxi Zhang, Fengjiang An, Shasha Liao, Cheng Wu, Jian Liu, and Yipeng Li. Study on numerical simulation methods for hypervelocity impact on large-scale complex spacecraft structures. *Aerospace*, 9:12–12, 12 2021.

[3] M. Wicklein, S. Ryan, D.M. White, and R.A. Clegg. Hypervelocity impact on cfrp: Testing, material modelling, and numerical simulation. *International Journal of Impact Engineering*, 35:1861–1869, 12 2008.

[4] Ngoc San Ha, Thong M. Pham, Tung T. Tran, Hong Hao, and Guoxing Lu. Mechanical properties and energy absorption of bio-inspired hierarchical circular honeycomb. *Composites Part B: Engineering*, 236:109818, 05 2022.

[5] K. Tewari, M. K. Pandit, P. R. Budarapu, and S. Natarajan. Analysis of sandwich structures with corrugated and spiderweb-inspired cores for aerospace applications. *Thin-Walled Structures*, 180:109812, 11 2022.

[6] Bianca Omede and Antonio Mattia Grande. Parametric optimization of bio-inspired engineered sandwich core. *Materials today communications*, 39:108632–108632, 03 2024.

[7] Qiancheng Zhang, Xiaohu Yang, Peng Li, Guoyou Huang, Shangsheng Feng, Cheng Shen, Bin Han, Xiaohui Zhang, Feng Jin, Feng Xu, and Tian Jian Lu. Bioinspired engineering of honeycomb structure – using nature to inspire human innovation. *Progress in Materials Science*, 74:332–400, 10 2015.

[8] Victoria Fisher. Unwinding the web: The mathematical basis of the spider web. *The Synapse: Intercollegiate science magazine*, 20, 01 2019.

[9] R.E. Skelton, R. Adhikari, J.-P. Pinaud, Waileung Chan, and J.W. Helton. An introduction to the mechanics of tensegrity structures. *Proceedings of the 40th IEEE Conference on Decision and Control (Cat. No.01CH37228)*, 5:4254–4259, 2001.

[10] Daniel Tinello, Dirk Jodin, and Herwig Winkler. Biomimetics applied to factory layout planning: Fibonacci based patterns, spider webs and nautilus shell as bio-inspiration to reduce internal transport costs in factories. *CIRP Journal of Manufacturing Science and Technology*, 13:51–71, 05 2016.

[11] Qiang He, Jun Feng, Yunjiang Chen, and Honggen Zhou. Mechanical properties of spider-web hierarchical honeycombs subjected to out-of-plane impact loading. *Journal of Sandwich Structures Materials*, 22:771–796, 04 2018.

[12] Afaf M. Abd El-Hameed and Y. A. Abdel-Aziz. Aluminium alloys in space applications: A short report. *Journal of Advanced Research in Applied Sciences and Engineering Technology*, 22:1–7, 01 2021.

[13] Shuang–Shuang Li, Xin Yue, Qing–Yuan Li, He–Li Peng, Bai–Xin Dong, Tian–Shu Liu, Hong–Yu Yang, Jun Fan, Shi–Li Shu, Feng Qiu, and Qi–Chuan Jiang. Development and applications of aluminum alloys for aerospace industry. *Journal of Materials Research and Technology*, 27:944–983, 11 2023.

[14] R Jini Raj, P. Panneer Selvam, and M. Pughalendi. A review of aluminum alloys in aircraft and aerospace industry, 06 2021.

[15] Matweb. Aluminium 7075 t6 datasheet.

[16] Peek carbon fibre reinforced - tecapeek cf30 black | ensinger, 2025.

[17] Yu Ye, Zixin Yang, Dianwei Qu, Bingyin Hu, and Lei Li. Orthotropic constitutive modeling and tsai–wu

failure criterion for carbon fiber-reinforced peek composites. *Polymers*, 17:1076–1076, 04 2025.

[18] Ankang Liu, Yunlong Chen, Jiqiang Hu, Bing Wang, and Li Ma. Low-velocity impact damage and compression after impact behavior of cf-peek thermoplastic composite laminates. *Polymer Composites*, 43:8136–8151, 08 2022.

[19] Li, Zhao, Li, Yang, and Wang. Flexural properties and fracture behavior of cf/peek in orthogonal building orientation by fdm: Microstructure and mechanism. *Polymers*, 11:656, 04 2019.

[20] Vidyasagar Matta, J Suresh Kumar, Duddu Venkataraviteja, and Guggulla Bharath Kumar Reddy. Flexural behavior of aluminum honeycomb core sandwich structure. *IOP Conference Series: Materials Science and Engineering*, 197:012046, 05 2017.

[21] Erdem TUNCA and Haşim Kafalı. Compression and three-point bending analyzes of aerospace sandwich composites produced with polymeric core materials with ansys. *Europan journal of science and technology*, 12 2021.

[22] B Muralidharan, S Kanmani Subbu, Arjun K Ajikumar, THEJESSHANAND KOONAPALLI, and S. Sasidharan. Experimental and numerical study of three-point bending test in five different fdm 3d printed pla core with carbon fiber sandwich structures. *Engineering Research Express*, 03 2025.

[23] Meiqin Liang, Shang Wang, and Fei Peng. Simulation and analysis of three-point bending experiment with hollow beam based on abaqus. *Journal of Physics: Conference Series*, 2566:012063, 08 2023.

[24] K. Toradmal, P. Waghmare, and S. Sollapur. Three point bending analysis of honeycomb sandwich panels: Experimental approach., 2017.

[25] Shanshan Shi, Zhi Sun, Xiaozhi Hu, and Haoran Chen. Flexural strength and energy absorption of carbon-fiber–aluminum-honeycomb composite sandwich reinforced by aluminum grid. *Thin-walled structures*, 84:416–422, 11 2014.

[26] Muzamil Hussain, Rafiullah Khan, and Naseem Abbas. Experimental and computational studies on honeycomb sandwich structures under static and fatigue bending load. *Journal of King Saud University - Science*, 31:222–229, 04 2019.